

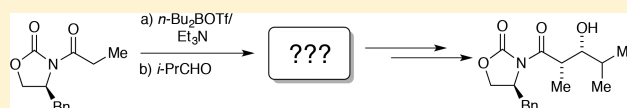
# Evans Enolates: Structures and Mechanisms Underlying the Aldol Addition of Oxazolidinone-Derived Boron Enolates

Zirong Zhang<sup>1b</sup> and David B. Collum<sup>\*1b</sup>

Department of Chemistry and Chemical Biology Baker Laboratory, Cornell University, Ithaca, New York 14853–1301, United States

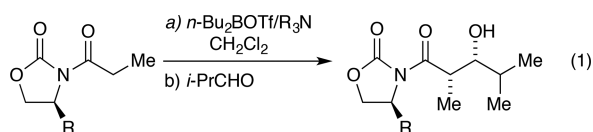
**S** Supporting Information

**ABSTRACT:** The soft enolization of an acylated oxazolidinone using di-*n*-butylboron triflate (*n*-Bu<sub>2</sub>BOTf) and trialkylamines and subsequent aldol addition was probed structurally and mechanistically using a combination of IR and NMR spectroscopies. None of the species along the reaction coordinate show a penchant for aggregating. Complexation of the acylated oxazolidinone by *n*-Bu<sub>2</sub>BOTf was too rapid to monitor, as was the subsequent enolization with Et<sub>3</sub>N (triethylamine). The preformed *n*-Bu<sub>2</sub>BOTf·Et<sub>3</sub>N complex, displaying muted Lewis acidity and affiliated tractable rates, reveals a rate-limiting complexation via a transition structure with a complicated counterion. *n*-Bu<sub>2</sub>BOTf·*i*-Bu<sub>3</sub>N bearing a hindered amine shifts the rate-limiting step to proton transfer. Rate studies show that the aldol addition with isobutyraldehyde occurs as proffered by others.



## INTRODUCTION

During the development of polyketide total syntheses and the emergence of biomimetic aldol additions, few reagents have been as central as the oxazolidinone enolates, colloquially referred to as Evans enolates.<sup>1</sup> In their seminal 1981 paper, Evans and co-workers<sup>2</sup> showed that the acylated oxazolidinone scaffold controls additions with high facial selectivity. Although their first attempts likely involved alkali-metal enolates, boron enolates derived from di-*n*-butylboron triflate<sup>3</sup> (*n*-Bu<sub>2</sub>BOTf) provide exceptional diastereoselectivities (eq 1).<sup>4</sup> Since that first publication, Evans enolates have been reported in an astonishing 1600 patents.<sup>5</sup>



Boron enolates, including several derived from oxazolidinones,<sup>6</sup> have been examined crystallographically,<sup>7</sup> spectroscopically,<sup>7,8</sup> and computationally.<sup>9,10</sup> By contrast, few experimental probes of mechanism have been carried out with either simple boron enolates<sup>11</sup> or oxazolidinone-based variants.<sup>6,12–15</sup> On the heels of investigations of lithium-based aldol additions of Evans enolates,<sup>12</sup> we undertook structural and mechanistic studies of the boron variant in Scheme 1.<sup>16</sup>

## RESULTS

**Structure Determinations: General Strategies.** The aldol addition was carried out as prescribed in the literature;<sup>2</sup> however, CHCl<sub>3</sub> was used interchangeably with CH<sub>2</sub>Cl<sub>2</sub> owing to the convenience of CDCl<sub>3</sub> for <sup>1</sup>H and <sup>13</sup>C NMR spectroscopies. <sup>11</sup>B NMR spectroscopy was ineffectual, owing to broad, poorly resolved resonances. IR spectroscopy, by contrast, proved particularly informative; carbonyl absorbances

of key species are summarized in Table 1. Representative IR spectra are contained in Figure 1. <sup>1</sup>H and <sup>13</sup>C NMR spectroscopies were used to confirm the structures of key species (Supporting Information).

**Table 1.** IR Absorbances of Key Intermediates<sup>a</sup>

compd	C=X (cm <sup>-1</sup> )	
1	1777	1704
2	1777	1704
3	1727 <sup>b</sup>	
4	1706	1658
6	1777	1704

<sup>a</sup>1777 and 1704 correspond to the oxazolidinone and propionyl group carbonyls, respectively.<sup>14,15</sup> <sup>b</sup>Superimposed single absorbance.

The method of continuous variations (MCV) was used to ascertain whether key intermediates associate into higher aggregates that would otherwise go undetected with standard spectroscopic methods.<sup>17</sup> If boron enolates are dimeric in solution, binary mixtures of two structurally related enolates would contain homodimers, A<sub>2</sub> and B<sub>2</sub>, and a heterodimer, AB (eq 2). AB would appear as a new species or, in the event of rapid exchange, elicit changes in time-averaged <sup>1</sup>H or <sup>13</sup>C NMR chemical shifts. In the event, numerous binary mixtures of complexes (3), enolates (4), or alkoxides (6) derived from substrates in Chart 1 showed no evidence of AB.



**Complexation.** The addition of 1.0 equiv of *n*-Bu<sub>2</sub>BOTf to oxazolidinone 1 (0.10 M in CHCl<sub>3</sub>) at 20 °C resulted in approximately 50% consumption of 1 and the appearance of a

Received: June 2, 2017

Published: July 7, 2017

Scheme 1. Mechanism of Oxazolidinone-Based Aldol Addition

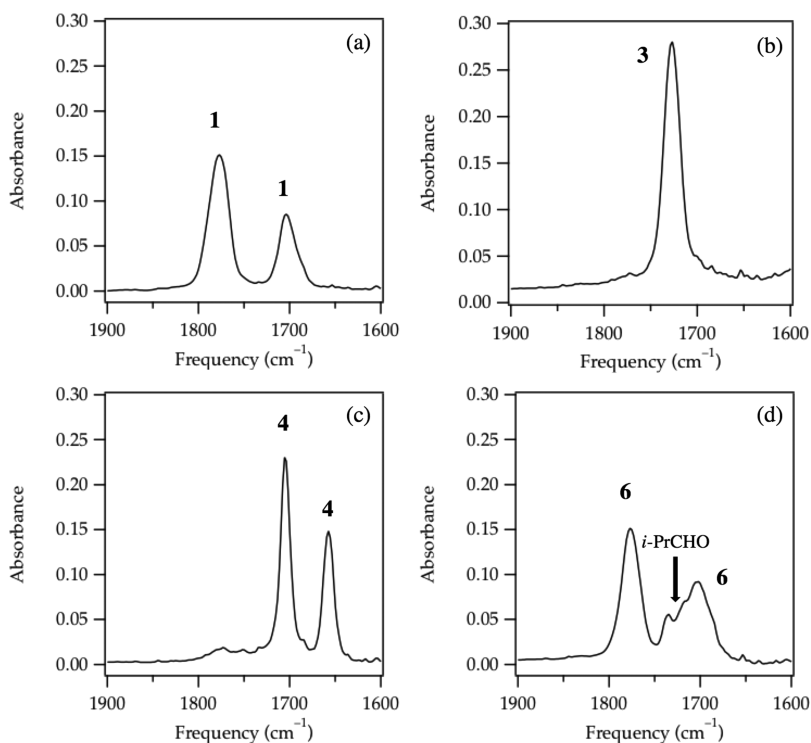
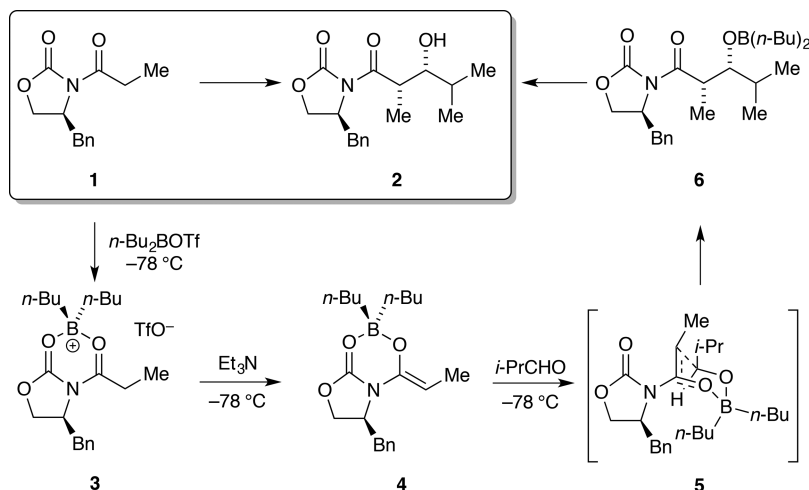
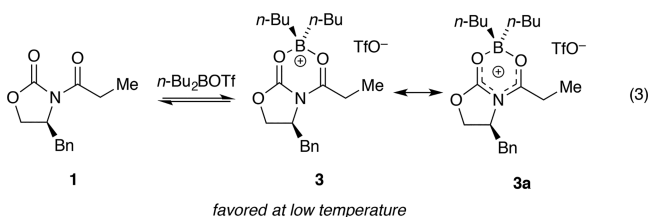


**Figure 1.** IR spectra of 0.10 M **1** in  $\text{CHCl}_3$  recorded at  $-60^\circ\text{C}$  with (a) no additive; (b) 0.11 M  $n\text{-Bu}_2\text{BOTf}$ , affording **3**; (c) 0.11 M  $n\text{-Bu}_2\text{BOTf}$  and 0.12 M  $\text{Et}_3\text{N}$ , affording **4**; and (d) 0.11 M  $n\text{-Bu}_2\text{BOTf}$ , 0.12 M  $\text{Et}_3\text{N}$ , and 0.13 M  $i\text{-PrCHO}$ , affording **6**.

single new absorbance at  $1727\text{ cm}^{-1}$  corresponding to complex **3**. We suspect that the electron distribution exemplified by resonance structure **3a** (eq 3) accounts for the single  $\text{C}=\text{X}$  absorbance.

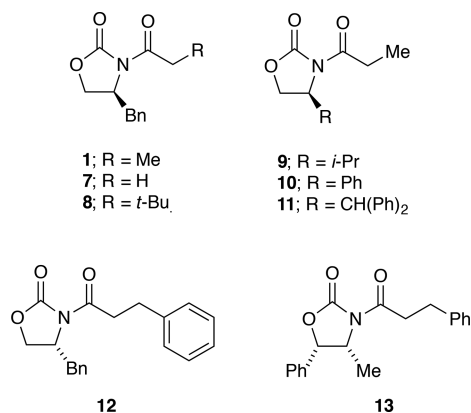


The reaction was instantaneous but not quantitative. Complete complexation was observed when the samples were

either cooled with 1.1 equiv  $n\text{-Bu}_2\text{BOTf}$  to  $-60^\circ\text{C}$  or combined with  $>3.0$  equiv of  $n\text{-Bu}_2\text{BOTf}$  at  $20^\circ\text{C}$  (vide infra).

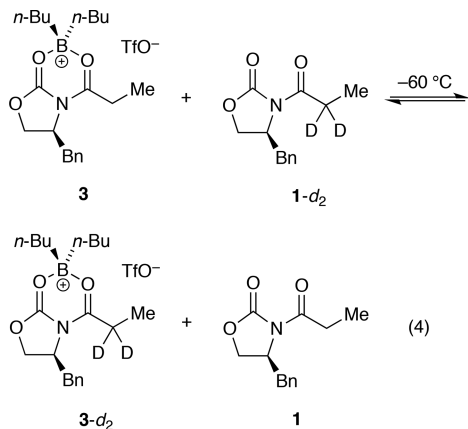
$^1\text{H}$  NMR spectroscopy showed the two diastereotopic protons of the propionyl methylene fragment in **3** as doublets of quartets with markedly different chemical shifts ( $\delta$  3.0 and 1.7 ppm). In partially complexed samples containing only 1.0 equiv of  $n\text{-Bu}_2\text{BOTf}$ , the upfield resonance appeared at 1.7 ppm at  $20^\circ\text{C}$  and shifted to 1.4 ppm at  $-60^\circ\text{C}$ . It would be tempting to ascribe this result to complexation promoted at low temperature, but the shift occurred independent of the  $n\text{-Bu}_2\text{BOTf}$  concentration, which also promoted complexation. We suspect that the temperature dependence stems from an aromatic  $\pi$ -interaction with the proximate  $\alpha$ -proton.<sup>18,19</sup> The analogous complex derived from **9**, which bears an isopropyl moiety, showed no anomalous shifting. Density functional

Chart 1. Enolate Precursors



theory (DFT) computations<sup>20</sup> for **3** with geometries optimized at the B3LYP/6-31G(d) level and corrected by single-point calculations at the MP2/6-31G(d)//B3LYP/6-31G(d) level did *not* support a proton–arene interaction.

Slow exchange on <sup>1</sup>H and <sup>13</sup>C NMR time scales made the two magnetically inequivalent *n*-butyl groups of **3** discernible. The treatment of complex **3** with **1-d<sub>2</sub>** showed rapid incorporation at –60 °C on <sup>1</sup>H NMR spectroscopy (eq 4), confirming that exchange was fast on laboratory time scales.



The results of <sup>19</sup>F NMR spectroscopy at –60 °C showed a single resonance ( $\delta$  –77 ppm) consistent with a free triflate ion that shifted downfield with additional *n*-Bu<sub>2</sub>BOTf. By comparison, CF<sub>3</sub>SO<sub>3</sub>H and *n*-Bu<sub>2</sub>BOTf displayed <sup>19</sup>F resonances at –79 and –76 ppm, respectively. The triflate counterion story becomes much more complicated.

**Enolization.** Adding triethylamine (Et<sub>3</sub>N; 1.2 equiv) to solutions containing >95% complex **3** (1.1 equiv of *n*-Bu<sub>2</sub>BOTf, –60 °C) afforded enolate **4** instantaneously and quantitatively, as shown by the replacement of the absorbance of **3** with two new C=X absorbances (Table 1). Chelation by the oxazolidinone carbonyl was evidenced by the lower energy carbonyl absorbance at 1706 cm<sup>–1</sup> (Table 1). The magnetically inequivalent *n*-butyl moieties of **4**, however, were time-averaged in the <sup>1</sup>H and <sup>13</sup>C NMR spectra at –60 °C, suggesting weak chelation.

**Tandem Complexation–Enolization.** The complexation of **1** to form **3** was too fast to monitor, as was the enolization of **3** to form enolate **4**. However, **1** reacted with a preassociated *n*-Bu<sub>2</sub>BOTf·Et<sub>3</sub>N complex at 0 °C at tractable rates with no detectable precomplex **3** owing to the attenuated (inhibited)

Lewis acidity.<sup>21</sup> *n*-Bu<sub>2</sub>BOTf·Et<sub>3</sub>N reacted in slow exchange with free Et<sub>3</sub>N, and the <sup>1</sup>H NMR spectra confirmed the 1:1 complex noted previously.<sup>22,23</sup>

Rate studies revealed both expected and decidedly unexpected results. The conversion of **1** to enolate **4** at 0 °C under pseudo-first-order conditions (0.0020 M **1**) followed a first-order decay, as confirmed by pseudo-first-order rate constants (*k*<sub>obsd</sub>) that were independent of the concentration of **1**. Comparing **1** and **1-d<sub>2</sub>** afforded no isotope effect (*k*<sub>H</sub>/*k*<sub>D</sub> = 1.00 ± 0.01). Post-rate-limiting enolization was confirmed by two additional experiments.<sup>24</sup> A mixture of preformed complexes **3** and **3-d<sub>2</sub>** (1.0 equiv each) was treated with a deficiency (0.80 equiv) of Et<sub>3</sub>N, thereby forcing the instantaneous deprotonation to select H over D. The selective loss of **3** monitored with <sup>1</sup>H NMR spectroscopy showed a large competitive isotope effect (*k*<sub>H</sub>/*k*<sub>D</sub> = 10). To confirm that the deprotonation of **3** was faster than decomplexation—a requirement for post-rate-limiting proton transfer<sup>24</sup>—we added low concentrations of an equimolar mixture of **1-d<sub>2</sub>** and Et<sub>3</sub>N to a solution of **3**. Enolization proceeded to the exclusion of the exchange of **1-d<sub>2</sub>** into **3**. Conversely, adding low concentrations of an equimolar mixture of **1** and Et<sub>3</sub>N to a solution of **3-d<sub>2</sub>** again resulted in dominant enolization, with approximately 10% incorporation of **1** into complex **3-d<sub>2</sub>**. Slowing the isotopically sensitive enolization 10-fold relative to exchange with substrate revealed a 10% competing back-reaction, which would have gone undetected in a measured isotope effect.<sup>24</sup>

A plot of *k*<sub>obsd</sub> versus Et<sub>3</sub>N concentration in excess showed an approximate inverse-first-order dependence (*n* = –0.9 ± 0.1) consistent with the reversible loss of the amine from *n*-Bu<sub>2</sub>BOTf·Et<sub>3</sub>N (Figure 2). Quite unexpectedly, a plot of *k*<sub>obsd</sub>

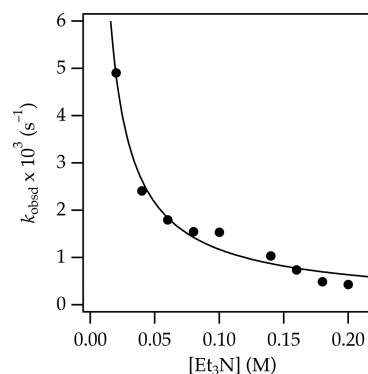


**Figure 2.** Plot of *k*<sub>obsd</sub> versus added Et<sub>3</sub>N concentration for the enolization of **1** (0.0020 M) by *n*-Bu<sub>2</sub>BOTf·Et<sub>3</sub>N (0.040 M) in CHCl<sub>3</sub> at 0 °C. *y* = *ax*<sup>*b*</sup>, *a* = 0.00015 ± 0.00003, *b* = –0.88 ± 0.05.

versus *n*-Bu<sub>2</sub>BOTf·Et<sub>3</sub>N concentration in which the excess amine concentration was held constant showed a *third-order dependence* (*n* = 3.3 ± 0.3; Figure 3). We neither anticipated this result nor have a fully satisfactory explanation, as discussed below.

$$-d[\mathbf{1}]/dt = k'[\mathbf{1}][n\text{-Bu}_2\text{BOTf}\cdot\text{Et}_3\text{N}]^3[\text{Et}_3\text{N}]^{-1} \quad (5)$$

Taken together, the reaction orders afforded the rate law in eq 5, which implicated a transition structure with [(**1**)(*n*-Bu<sub>2</sub>BOTf)<sub>3</sub>(Et<sub>3</sub>N)<sub>2</sub>]<sup>‡</sup> stoichiometry.<sup>25</sup> The triflate-based counterion denoted as “X<sup>–</sup>” at the transition state would necessarily be complicated. Neither of the two amines in the rate-limiting transition state served as a Brønsted base because

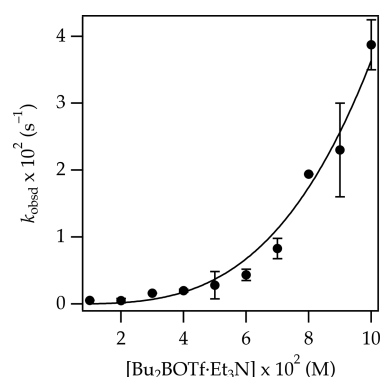
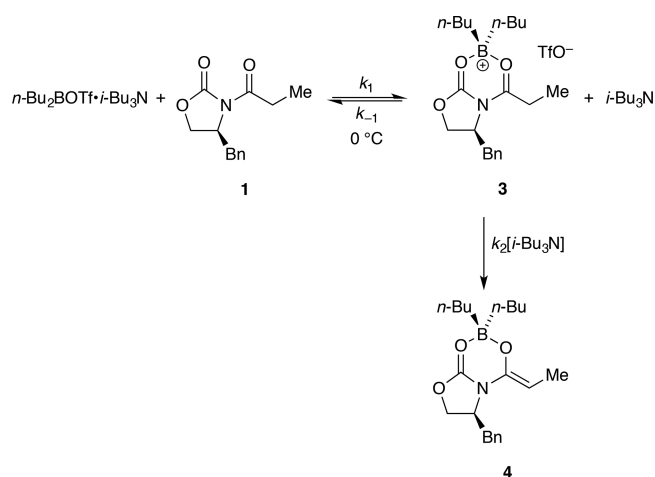


**Figure 3.** Plot of  $k_{\text{obsd}}$  versus  $n\text{-Bu}_2\text{BOTf}\cdot\text{Et}_3\text{N}$  concentration for the enolization of **1** (0.0020 M) by 0.10 M free (uncomplexed)  $\text{Et}_3\text{N}$  in  $\text{CHCl}_3$  at 0 °C.  $y = ax^b$ ,  $a = 72 \pm 3$ ,  $b = 3.3 \pm 0.3$ .

the deprotonation is post-rate-limiting. We defer the interpretation of stoichiometry to the **Discussion**; however, we probed the amine dependence and obtained the following relative reaction rates:  $\text{Me}_2\text{NEt}$  (DMEA) <  $\text{MeNEt}_2$  <  $\text{Et}_3\text{N}$  <  $i\text{-Pr}_2\text{NEt}$  <  $i\text{-Bu}_3\text{N}$ .

$i\text{-Bu}_3\text{N}$  shifted the equilibrium to nonlimiting behavior that has the effect of shifting the rate-limiting step to proton transfer, as described by **Scheme 2** and eqs 6–9. A plot of  $k_{\text{obsd}}$

### Scheme 2. Competitive Amine-Mediated Complexation and Enolization



versus  $i\text{-Bu}_3\text{N}$  concentration showed saturation kinetics (**Figure 4**) in which substrate and  $i\text{-Bu}_3\text{N}$  competitively coordinate to boron.  $K_{\text{eq}}$  was commensurate with a value measured with  $^1\text{H}$  NMR using enolization-resistant isobutyrate **21** (see below) as a surrogate. The enolization of **1** using  $i\text{-Bu}_3\text{N}$  showed rate-limiting proton transfer, as evidenced by a large kinetic isotope effect ( $k_{\text{H}}/k_{\text{D}} = 10$ ) at low and high amine concentrations. Changing the addition sequence by adding  $i\text{-Bu}_3\text{N}$  to the substrate–boron complex provided the same behavior. The counterintuitive normal (rather than inverse) saturation owing to an unproductive side equilibrium stemmed from the dual role of amine as both inhibiting Lewis base and accelerating Brønsted base.

$$d[\mathbf{4}]/dt = k_{\text{obsd}}[\mathbf{1}_{\text{total}}] \quad (6)$$

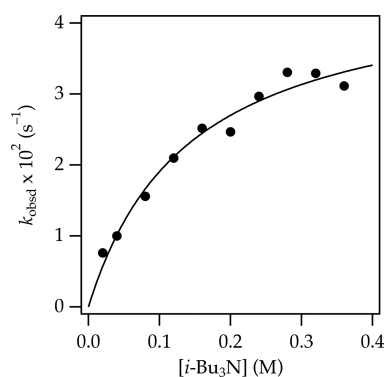


**Figure 4.** Plot of  $k_{\text{obsd}}$  versus  $i\text{-Bu}_3\text{N}$  concentration for the enolization of **1** (0.0020 M) by  $n\text{-Bu}_2\text{BOTf}\cdot i\text{-Bu}_3\text{N}$  (0.040 M) and  $i\text{-Bu}_3\text{N}$  in  $\text{CHCl}_3$  at 0 °C.  $y = ax/(x + b)$ ,  $a = 0.046 \pm 0.004$ ,  $b = 0.14 \pm 0.03$ .

$$k_{\text{obsd}} = k_2 K_{\text{eq}} [n\text{-Bu}_2\text{BOTf}\cdot i\text{-Bu}_3\text{N}] / \{1 + K_{\text{eq}} [n\text{-Bu}_2\text{BOTf}\cdot i\text{-Bu}_3\text{N}] / [i\text{-Bu}_3\text{N}]\} \quad (7)$$

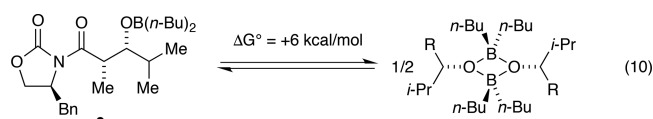
low amine concentration:

$$k_{\text{obsd}} = k_2 [i\text{-Bu}_3\text{N}] \quad (8)$$

high amine concentration:

$$k_{\text{obsd}} = k_2 K_{\text{eq}} [n\text{-Bu}_2\text{BOTf}\cdot i\text{-Bu}_3\text{N}] \quad (9)$$

**Aldol Addition.** The reaction of enolate **4** (0.10 M) and excess  $\text{Et}_3\text{N}$  (0.020 M) with  $i\text{-PrCHO}$  (0.13 M) in  $\text{CH}_2\text{Cl}_2$  at  $-78$  °C afforded adduct **6** at tractable rates. The absence of chelation in alkoxide **6** was shown by carbonyl absorbances that were nearly indistinguishable from those of starting oxazolidinone **1**. The absence of aggregation was shown experimentally using MCV (vide supra) and supported by DFT computations predicting the dimerization of alkoxide **6** (eq 10) to be highly endothermic.<sup>26</sup>



Reactions under pseudo-first-order conditions (0.0050 M enolate **4** and 0.050 M  $i\text{-PrCHO}$ ) showed first-order decays of enolate and  $k_{\text{obsd}}$  values that were independent of the initial enolate concentration (**Figure 5**). The rate was unaffected by excess  $\text{Et}_3\text{N}$  or added tetrahydrofuran. The rate law in eq 11

$$-d[\mathbf{4}]/dt = k'[\mathbf{4}][i\text{-PrCHO}] \quad (11)$$

is consistent with a simple aldol addition mechanistically akin to that proposed by Evans in the original work (**5** in **Scheme 1**). DFT studies mirroring those reported by Kobayashi and co-workers<sup>6</sup> showed transition structure **5a** to be both viable and 4.7 kcal/mol more stable than transition structure **5b** leading to the wrong isomer.<sup>1,2</sup>

## DISCUSSION

The structural and mechanistic studies of the Evans boron aldol addition proceeded largely according to conventional wisdom. Treating oxazolidinone **1** at 20 °C with  $n\text{-Bu}_2\text{BOTf}$  causes the instantaneous formation of complex **3**. Full complexation requires cooling to  $-60$  °C or the use of excess  $n\text{-Bu}_2\text{BOTf}$  at

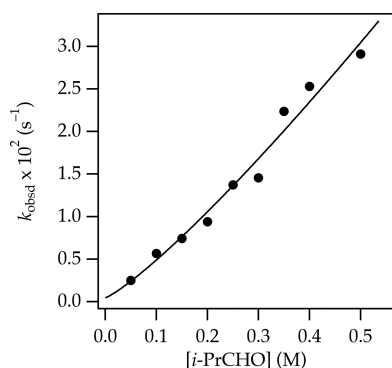
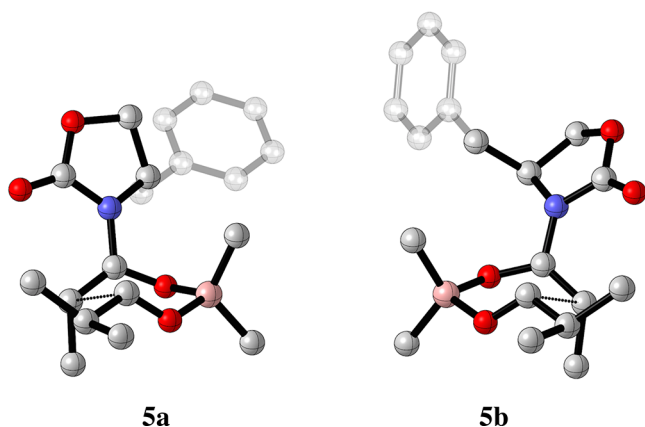


**Figure 5.** Plot of  $k_{\text{obsd}}$  versus *i*-PrCHO concentration for aldol addition by enolate **4** (0.0050 M) with a slight (0.0010 M) excess of  $\text{Et}_3\text{N}$  in  $\text{CHCl}_3$  at  $-60^\circ\text{C}$ .  $y = ax^b$ ,  $a = 0.067 \pm 0.007$ ,  $b = 1.09 \pm 0.10$ .



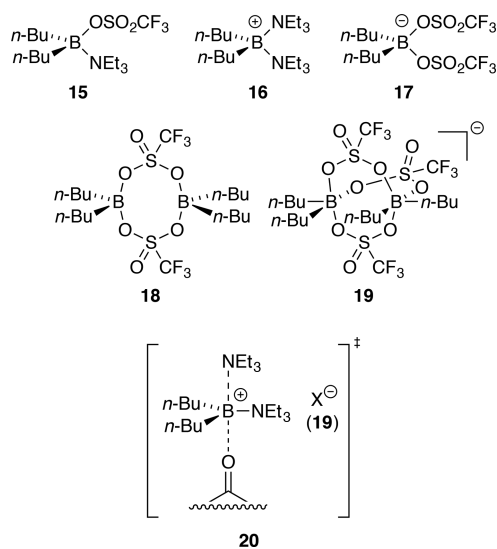
$20^\circ\text{C}$ . Treatment of **3** with trialkylamines at  $-78^\circ\text{C}$  effects instantaneous enolization to give boron enolate **4**. Aldol addition to *i*-PrCHO at  $-60^\circ\text{C}$  affords boron alkoxide **6**.

IR spectroscopy provided compelling support for the chelates in **3** and **4**, whereas the carbonyl of **6** does not coordinate to boron. Computations were in full accord with the monomeric alkoxide **6**.<sup>26</sup> MCV also provided no evidence that **3**, **4**, or **6** aggregate.

The high rates of complexation and enolization were overcome using *n*-Bu<sub>2</sub>BOTf·Et<sub>3</sub>N mixtures, which caused a marked attenuation of the complexation rate. The rate studies confirmed a rate-limiting complexation followed by rapid (post-rate-limiting) enolization. The success of the standard boron aldol addition stems from the fact that the incomplete **1**–**3** equilibrium is driven to enolate **4** by the enolization. Switching to *n*-Bu<sub>2</sub>BOTf·*i*-Bu<sub>3</sub>N displaces the equilibrium toward observable complex **3** and shifts the rate-limiting step to proton transfer (Scheme 2).<sup>23</sup>

The details of the complexation are very odd. Although complex **3** represents a simple  $\text{CF}_3\text{SO}_3^-$  (“X<sup>−</sup>”), a third-order dependence on *n*-Bu<sub>2</sub>BOTf·Et<sub>3</sub>N in conjunction with an inverse-first-order dependence on amine implicates a rate-limiting transition structure with an unexpected [(*n*-Bu<sub>2</sub>BOTf)<sub>3</sub>(Et<sub>3</sub>N)<sub>2</sub>]<sup>‡</sup> stoichiometry.<sup>25,27</sup> Chart 2 shows a number of fragments—possible building blocks—that could be in play, ranging from highly plausible to merely conceivable. The titration of *n*-Bu<sub>2</sub>BOTf with Et<sub>3</sub>N clearly shows a 1:1 complex consistent with **15**. A single *n*-Bu group excludes the ion pair of **16** and **17**. Dimer **18** is supported by limited literature precedent,<sup>28</sup> but it offers us nothing useful. The 3:2 stoichiometry demands a reactive form such as that composed

**Chart 2.** Possible Boron-Containing Fragments



of Lewis acidic **16** and counterion **19** with five-coordinate borons. The evidence of five-coordinate boron is sound.<sup>29</sup> We piece this together to create transition structure **20** for rate-limiting complexation. The five-coordinate, trigonal bipyramidal substitution at boron has strong precedent from some rate studies we did a dozen years ago on imine activation by  $\text{BF}_3\text{--R}_3\text{N}$  complexes.<sup>30</sup> The complex geogion remains the controversial portion. And, as a referee noted, if the third-order dependence in Figure 3 is actually a second-order dependence that is in error—it happens—one can replace geogion **19** with the far more conventional **17**. It would be an understatement to say that we are uneasy about parts of the model.

As an aside, the kinetics using the *n*-Bu<sub>2</sub>BOTf·*i*-Pr<sub>2</sub>NEt bearing a more hindered trialkylamine to form enolate **4** shows a 30-fold acceleration relative to the rates with the Et<sub>3</sub>N variant, as expected for a mechanism requiring an amine dissociation. Interestingly, the measured reaction order in *n*-Bu<sub>2</sub>BOTf·*i*-Pr<sub>2</sub>NEt approaches unity ( $n = 1.3$ ). The complex counterion may be unfavorable if the cation fragment (analogous to **16**) becomes too congested.

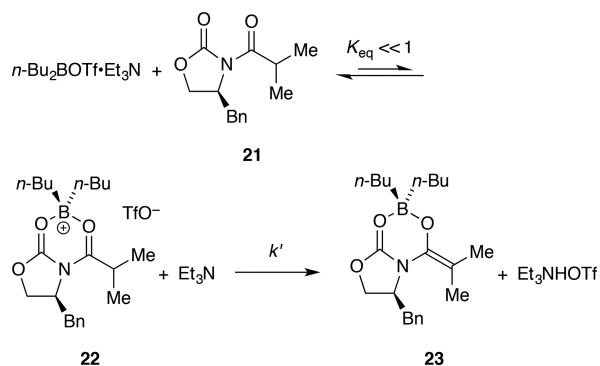
The final step—the aldol addition of **4** to give **6** via transition structure **5** (Scheme 1)—is mechanistically uneventful. Neither Et<sub>3</sub>N nor added tetrahydrofuran inhibits the reaction, which shows that the putative four-coordinate boron in **4** is undisturbed by Lewis basic ligands. Kobayashi and co-workers<sup>6</sup> carried out calculations probing the nuances of **5** and competing orientations. These calculations showed consistency in the open transition structure and approach with the aldehyde anti to the benzyl group.

## CONCLUSION

We described studies of the boron enolate-based Evans aldol addition. The most surprising aspect proves to be the mechanism of complexation, in which we may have uncovered some unusual organoboron coordination chemistry. The potentially most useful part, however, is probably the insights gained about the dual role of trialkylamines as inhibitors—complexants to the Lewis acid—and Bronsted bases. Suspecting that we could use this information to optimize the quaternization of the  $\alpha$ -carbon using boron enolates,<sup>4</sup> we formed complex **22** from isobutyryl derivative **21**. The addition



of Et<sub>3</sub>N pushes the equilibrium to **21** rather than enolate **23**, however. More hindered trialkylamines promote complexation but are too unreactive as Brønsted bases. Thus, the quaternization faces challenges posed by such soft enolization methods.



It seems generally useful, even advisable, to understand the structural and mechanistic principles underlying synthetically prevalent reactions such as the Evans aldol addition.

## EXPERIMENTAL SECTION

**Reagents and Solvents.** CH<sub>2</sub>Cl<sub>2</sub>, CHCl<sub>3</sub>, and CDCl<sub>3</sub> were distilled from molecular sieves. Trialkylamines were distilled from sodium benzophenone ketyl. *n*-Bu<sub>2</sub>BOTf was used as a neat oil by evaporating the solvent from a commercial 1.0 M *n*-Bu<sub>2</sub>BOTf solution in CH<sub>2</sub>Cl<sub>2</sub>. Air- and moisture-sensitive materials were manipulated under argon using standard glovebox, vacuum line, and syringe techniques. Oxazolidinones **1** and **7–13** were either purchased or prepared as described previously.<sup>31</sup>

**NMR Spectroscopy.** An NMR tube under vacuum was flame-dried on a Schlenk line and allowed to return to room temperature, backfilled with argon, and placed in a  $-78$  °C dry ice/acetone bath. The appropriate amounts of *n*-Bu<sub>2</sub>BOTf, Et<sub>3</sub>N, and oxazolidinone in CDCl<sub>3</sub> were added sequentially via syringe. The tube was flame-sealed under partial vacuum, mixed on a vortex mixer three times for  $\sim 10$  s with cooling between each vortexing, and stored in a freezer at  $-80$  °C. Standard <sup>1</sup>H, <sup>13</sup>C, and <sup>19</sup>F NMR spectra were recorded on a 500 MHz spectrometer at 500, 125, and 470 MHz, respectively. The <sup>1</sup>H, <sup>13</sup>C, and <sup>19</sup>F resonances are referenced to CDCl<sub>3</sub> (CHCl<sub>3</sub> 7.26 and CDCl<sub>3</sub> 77.16 ppm) and fluorobenzene ( $-113.15$  ppm).

**IR Spectroscopic Analyses.** IR spectra were recorded with an in situ IR spectrometer fitted with a 30-bounce, silicon-tipped probe. The spectra were acquired in 16 scans at a gain of 1 and a resolution of 4 cm<sup>-1</sup>. A representative reaction was carried out as follows: The IR probe was inserted through a nylon adapter and O-ring seal into an oven-dried, cylindrical flask fitted with a magnetic stir bar and a T-joint. The T-joint was capped with a septum for injections and a nitrogen line. After evacuation under full vacuum, heating, and flushing with nitrogen, the flask was charged with CHCl<sub>3</sub> and cooled in a  $-60$  °C bath prepared with fresh acetone. After a background spectrum was recorded, oxazolidinone **1** (23.3 mg, 0.10 mmol) was added as a 1.0 M solution in CHCl<sub>3</sub> with stirring, followed by neat *n*-Bu<sub>2</sub>OTf (30.2 mg, 0.11 mmol), neat Et<sub>3</sub>N (12.1 mg, 0.12 mmol), and *i*-PrCHO (9.4 mg, 0.13 mmol). IR spectra were recorded every 15 s with monitoring of the absorbance at 1777 and 1658 cm<sup>-1</sup> over the course of the reaction.

## ASSOCIATED CONTENT

### Supporting Information

The Supporting Information is available free of charge on the ACS Publications website at DOI: 10.1021/acs.joc.7b01365.

Spectra, kinetic and computational data, and authors for ref **20** (PDF)

## AUTHOR INFORMATION

### Corresponding Author

\*E-mail: dbc6@cornell.edu

### ORCID

Zirong Zhang: 0000-0002-6720-4644

David B. Collum: 0000-0001-6065-1655

### Notes

The authors declare no competing financial interest.

## ACKNOWLEDGMENTS

We thank the National Institutes of Health (GM077167) for support.

## REFERENCES

- (1) (a) Evans, D. A.; Shaw, J. T. *L'actualité Chimique* **2003**, 35. (b) Lin, G.-Q.; Li, Y.-M.; Chan, A. S. C. *Principles and Applications of Asymmetric Synthesis*; Wiley & Sons: New York, 2001; p 135. (c) *Modern Aldol Reactions*; Mahrwald, R., Ed.; Wiley-VCH: Weinheim, 2004; Vols. 1 and 2.
- (2) Evans, D. A.; Bartroli, J.; Shih, T. L. *J. Am. Chem. Soc.* **1981**, 103, 2127.
- (3) The term “triflate” derives from the University of California, Berkeley and was cinematically inspired by the science fiction movie *The Day of the Triffids*. Charles Wilkins, personal communication.
- (4) (a) Cowden, C. J.; Paterson, I. *Org. React.* **1997**, 51, 1. (b) Abiko, A. In *Boron Reagents in Synthesis*; ACS Symposium Series 1236; American Chemical Society: Washington, DC, 2016, p 123.
- (5) Evans, D. A.; Kim, A. S.; Skrydstrup, T.; Taaning, R. H. (*S*)-4-Benzyl-2-oxazolidinone; John Wiley & Sons, New York, 2007; pp 1–18.
- (6) (a) Makino, Y.; Iseki, K.; Fujii, K.; Oishi, S.; Hirano, T.; Kobayashi, Y. *Tetrahedron Lett.* **1995**, 36, 6527. (b) Shinisha, C. B.; Sunoj, R. B. *J. Am. Chem. Soc.* **2010**, 132, 12319. (c) Sreenithya, A.; Sunoj, R. B. *Org. Lett.* **2012**, 14, 5752. (d) Shinisha, C. B.; Sunoj, R. B. *Org. Lett.* **2010**, 12, 2868.
- (7) Ma, L.; Hopson, R.; Li, D.; Zhang, Y.; Williard, P. G. *Organometallics* **2007**, 26, 5834.
- (8) (a) Abiko, A.; Inoue, T.; Masamune, S. *J. Am. Chem. Soc.* **2002**, 124, 10759. (b) Bai, J.; Burke, L. D.; Shea, K. J. *J. Am. Chem. Soc.* **2007**, 129, 4981.
- (9) For selected recent computational studies of boron enolates, see the following: (a) Dias, L. C.; Pinheiro, S. M.; de Oliveira, V. M.; Ferreira, M. A. B.; Tormena, C. F.; Aguiar, A. M.; Zukerman-Schpector, J.; Tiekink, E. R. T. *Tetrahedron* **2009**, 65, 8714. (b) Paton, R. S.; Goodman, J. M. *J. Org. Chem.* **2008**, 73, 1253. (c) Dias, L. C.; de Lucca, E. C., Jr.; Ferreira, M. A. B.; Garcia, D. C.; Tormena, C. F. *J. Org. Chem.* **2012**, 77, 1765. (d) Paton, R. S.; Goodman, J. M. *Org. Lett.* **2006**, 8, 4299.
- (10) For a review of theoretical studies of boron enolates, see the following: Domingo, L. R.; Andres, J. In *The Chemistry of Metal Enolates*; Rappoport, Z., Ed.; Wiley: New York, 2009; Vol. 1, Chapter 1.
- (11) Cergol, K. M.; Jensen, P.; Turner, P.; Coster, M. J. *Chem. Commun.* **2007**, 1363.
- (12) (a) Tallmadge, E. H.; Collum, D. B. *J. Am. Chem. Soc.* **2015**, 137, 13087. (b) Tallmadge, E. H.; Jermaks, J.; Collum, D. B. *J. Am. Chem. Soc.* **2016**, 138, 345.
- (13) (a) Danda, H.; Hansen, M. M.; Heathcock, C. H. *J. Org. Chem.* **1990**, 55, 173. (b) Baringhaus, K.-H.; Matter, H.; Kurz, M. *J. Org. Chem.* **2000**, 65, 5031. (c) Evans, D. A.; Nelson, J. V.; Vogel, E.; Taber, T. R. *J. Am. Chem. Soc.* **1981**, 103, 3099. (d) Kimball, D. B.; Michalczyk, R.; Moody, E.; Ollivault-Shiflett, M.; De Jesus, K.; Silks, L. A., III *J. Am. Chem. Soc.* **2003**, 125, 14666.
- (14) Connolly, T. J.; Hansen, E. C.; MacEwan, M. F. *Org. Process Res. Dev.* **2010**, 14, 466.
- (15) A copper complex of an acylated oxazolidinone shows similar IR absorbances: (a) Evans, D. A.; Scheidt, K. A.; Johnston, J. N.; Willis,

M. C. *J. Am. Chem. Soc.* **2001**, *123*, 4480. (b) Evans, D. A.; Miller, S. J.; Lectka, T.; von Matt, P. *J. Am. Chem. Soc.* **1999**, *121*, 7559.

(16) For an excellent review of soft enolization, see the following: Evans, D. A.; Shaw, J. T. [http://isites.harvard.edu/fs/docs/icb.topic93502.files/Lectures\\_and\\_Handouts/25-Handouts/SoftEnolization\\_draft.pdf](http://isites.harvard.edu/fs/docs/icb.topic93502.files/Lectures_and_Handouts/25-Handouts/SoftEnolization_draft.pdf).

(17) Renny, J. S.; Tomasevich, L. L.; Tallmadge, E. H.; Collum, D. B. *Angew. Chem., Int. Ed.* **2013**, *52*, 11998.

(18) Martin, N. H.; Allen, N. W., III; Moore, K. D.; Vo, L. *J. Mol. Struct.: THEOCHEM* **1998**, *454*, 161.

(19) Evans invoked  $\pi$  stacking during oxazolidinone-derived enolate functionalizations: Evans, D. A.; Chapman, K. T.; Hung, D. T.; Kawaguchi, A. T. *Angew. Chem., Int. Ed. Engl.* **1987**, *26*, 1184.

(20) Frisch, M. J.; et al. *Gaussian Version 3.09*; revision A.1; Gaussian, Inc.: Wallingford, CT, 2009.

(21) Ma, Y.; Lobkovsky, E.; Collum, D. B. *J. Org. Chem.* **2005**, *70*, 2335.

(22) For NMR spectroscopic studies of  $\text{BF}_3/\text{R}_3\text{N}$  complexes, see the following: Hartman, J. S.; Yuan, Z.; Fox, A.; Nguyen, A. *Can. J. Chem.* **1996**, *74*, 2131.

(23) For a discussion and leading references to ligand substitutions of BR3 derivatives, see the following: Toyota, S.; Futawaka, T.; Asakura, M.; Ikeda, H.; Oki, M. *Organometallics* **1998**, *17*, 4155.

(24) For discussions of monitoring post-rate-limiting steps and the implications of rate limitation, see the following: (a) Simmons, E. M.; Hartwig, J. F. *Angew. Chem., Int. Ed.* **2012**, *51*, 3066. (b) Algera, R. F.; Gupta, L.; Hoepker, A. C.; Liang, J.; Ma, Y.; Singh, K. J.; Collum, D. B. *J. Org. Chem.* **2017**, *82*, 4513.

(25) The rate law provides the stoichiometry of the transition structure relative to that of the reactants: (a) Edwards, J. O.; Greene, E. F.; Ross, J. *J. Chem. Educ.* **1968**, *45*, 381. (b) Collum, D. B.; McNeil, A. J.; Ramirez, A. *Angew. Chem., Int. Ed.* **2007**, *46*, 3002.

(26) (a) Vorontsova, L. G.; Chizhov, O. S.; Vasil'ev, L. S.; Mikhailov, B. M. *Izvest. Akad. Nauk. SSSR* **1981**, 353. (b) Gursky, M. E.; Shashkov, A. S.; Mikhailov, B. M. *J. Organomet. Chem.* **1980**, *199*, 171.

(27) In the following, Evans traced the need for excess Lewis acid in soft enolizations to ate complexes. (a) Aluminum: Evans, D. A.; Allison, B. D.; Yang, M. G.; Masse, C. E. *J. Am. Chem. Soc.* **2001**, *123*, 10840. (b) Boron: Personal communication..

(28) (a) Jordan, E.; Lestel, L.; Boileau, S.; Cheradame, H.; Gandini, A. *Makromol. Chem.* **1989**, *190*, 267. (b) Papp, R.; Somoza, F. B.; Sieler, J.; Blaurock, S.; Hey-Hawkins, E. *J. Organomet. Chem.* **1999**, *585*, 127.

(29) (a) Miyamoto, K.; Yokota, Y.; Suefuji, T.; Yamaguchi, K.; Ozawa, T.; Ochiai, M. *Chem. - Eur. J.* **2014**, *20*, 5447. (b) Uruichi, M.; Yakushi, K.; Yamashita, Y. *J. Mater. Chem.* **2000**, *10*, 2716. (c) Chaudhuri, M. K.; Das, B. *Inorg. Chem.* **1985**, *24*, 2580. (d) Brownstein, S. *Can. J. Chem.* **1967**, *45*, 2403. (e) Koner, S.; Ghosh, A.; Chaudhuri, N. R. *Bull. Chem. Soc. Jpn.* **1990**, *63*, 2387.

(30) Aubrecht, K. B.; Winemiller, M. D.; Collum, D. B. *J. Am. Chem. Soc.* **2000**, *122*, 11084.

(31) For the oxazolidinones, see the following. (a) **8**: Evans, D. A.; Britton, T. C.; Dorow, R. L.; Dellaria, J. F. *Tetrahedron* **1988**, *44*, 5525. (b) **11**: Perry, M. A.; Trinidad, J. V.; Rychnovsky, S. D. *Org. Lett.* **2013**, *15*, 472. (c) **12**: Szostak, M.; Spain, M.; Eberhart, A. J.; Procter, D. J. *J. Am. Chem. Soc.* **2014**, *136*, 2268. (d) **13**: Evans, D. A.; Mathre, D. J.; Scott, W. L. *J. Org. Chem.* **1985**, *50*, 1830.